



# Debonding of Porous Coating: A Late Failure Mode of Uncemented, Partially Threaded Acetabular Components—Retrieval Analysis

Łukasz Łapaj<sup>1</sup> · Joanna Sulej-Chojnacka<sup>2</sup> · Justyna Rozwalka<sup>2</sup> · Abdulrahim Alaouir<sup>4</sup> · Tomasz Markiewicz<sup>1</sup> · Paweł Chodór<sup>1</sup>  · Jan Kiryluk<sup>5</sup> · Adrian Mróz<sup>6</sup> · Jan Zabrzyński<sup>3</sup>

Submitted: 23 November 2023 / in revised form: 24 May 2024 / Accepted: 30 May 2024  
© The Author(s) 2024

**Abstract** Titanium plasma-sprayed (TPS) porous coatings have been used in total hip arthroplasty for decades. They are considered reliable, and very few failure cases have been described so far. This retrieval study described a series of 20 acetabular components—where total or partial debonding occurred during in vivo use and aimed to explain the underlying failure mechanisms. Implants were examined using optical and electron microscopy (SEM), metallographic sections of retrievals were prepared while pathologic samples of periprosthetic tissues were examined for presence of wear debris. Data from metallographic slides indicated that debonding was initiated at free borders of the coating and tended to progress at the interface between the TPS layer and the shell. In some cases, total

debonding occurred leading material wear of both the TPS layer and acetabular shell leading to massive release of metallic debris and accelerated polyethylene wear in third body mechanism. SEM examination demonstrated that splats forming the TPS layer exhibited features suggesting a high temperature gradient between the plasma sprayed layer and the substrate material existed, leading to porosity of splats and suboptimal bonding strength. This study demonstrated that coating application parameters and certain design features (screw holes, fins) may promote long-term failure due to debonding. Surgeons should be aware of this complication as it is most likely underreported, while manufacturers should consider more rigorous pre-clinical testing as suboptimal coating bonding may result in failures during long-term clinical use.

✉ Paweł Chodór  
pchodor@orsk.pl

<sup>1</sup> Department of General Orthopaedics, Musculoskeletal Oncology and Trauma Surgery, Poznan University of Medical Sciences, 28 Czerwca 1956 r 135/147, 61-545 Poznań, Poland

<sup>2</sup> Łukasiewicz Research Network, Poznan Institute of Technology, Ewarysta Estkowskiego 6, 61-755 Poznań, Poland

<sup>3</sup> Faculty of Medicine, Nicolas Copernicus University, Toruń, Collegium Medicum in Bydgoszcz, Jagiellońska 13/15, 85-067 Bydgoszcz, Poland

<sup>4</sup> Poznan University of Medical Sciences, Fredry 10, 61-701 Poznań, Poland

<sup>5</sup> Department of Orthopedics, Traumatology and Hand Surgery, Medical University of Białystok, M. Skłodowskiej-Curie 24a, 15-276 Białystok, Poland

<sup>6</sup> Mechanical Engineering Institute, Collegium Mechanicum, The President Stanisław Wojciechowski Calisia University, 4th Nowy Świat Street, 62-800 Kalisz, Poland

**Keywords** coating · debonding · failure · fatigue · plasma spray · uncemented joint replacement

## Introduction

Contemporary uncemented joint replacements require biologic fixation to ensure long-term functioning, and this process can be achieved by bony ongrowth or ingrowth (Ref 1). Over the past few decades, clinical experiences have led to the development of several successful surface finishes that facilitate biologic fixation. Among these, plasma-sprayed porous titanium coatings are perhaps the most widely used clinically, with millions of femoral and acetabular components of total hip replacements (THR) utilizing them (Ref 2, 3). The coarse surface of such coatings enhances primary stability, and excellent long-term fixation of such components has been demonstrated in

many studies and data from arthroplasty registries in many countries (Ref 2-4).

Once osseointegration is achieved, the coating is subjected to repetitive cyclic loading during gait and other physical activities (Ref 5-8). This places immense strain on the interface between the porous coating and the base metal of the components. Moreover, developing porous coatings for medical applications is a challenging task, as the porous nature of these coatings makes them susceptible to residual stress, which negatively affects their bonding strength (Ref 9). To ensure sufficient durability of the implants, pre-clinical testing protocols have been implemented. Current ISO and FDA guidelines include fatigue testing, static shear, and tensile strength testing (Ref 10-12). Consequently, titanium plasma-sprayed coatings are widely regarded as highly durable and are rarely the cause of implant failure.

Despite these rigorous testing requirements, various types of porous coatings used clinically have been reported to fail in vivo. The most commonly described issue is shedding of sintered beads, predominantly in acetabular components, and debonding of plasma-sprayed hydroxyapatite (HA) coatings in femoral and acetabular components (Ref 13-16). There are also several papers focused on coating failures in titanium plasma-sprayed (TPS) acetabular components. Some case reports describe coating failure in acetabular components made of titanium alloys (Ref 17-19). Coating debonding has also been reported in CoCrMo acetabular components of joint resurfacing implants; in one study, this affected 3.5% of all implants (Ref 11, 20, 21).

Possible mechanisms leading to the failure of plasma-sprayed coatings used in orthopedic implants have been explored in laboratory settings. A major advantage of such studies lies in the ability use acoustic emission techniques to monitor the effect of various parameters on crack initiation and propagation, which ultimately lead to coating failure (Ref 5-7). It has been demonstrated that multiple parameters such as temperature gradients during coating application, thickness of the coating or surface roughness of the substrate material influence coating durability, with most fatigue failures occurring at the coating-surface interface (Ref 6, 8, 9, 22, 23).

Debonding of TPS and other coatings of arthroplasty implants occurring in vivo has been reported in the literature, however most authors described these cases as a rare complication causing the need for implant revision and did not examine the failed implants (Ref 11, 13-15, 18, 20, 21, 24). Remarkably few studies exist where a detailed retrieval analysis was conducted and data from these papers is limited as they included a small number of samples (Ref 19, 20). However, in recent years, the authors have revised a series of acetabular cups with varying extent of coating failures, which offered an opportunity to

investigate the underlying causes. The present study examined this series of implants to determine the mechanisms of in vivo coating debonding.

## Materials and Methods

This study analyzed a series of 20 retrieved acetabular components with partial or complete debonding of TPS osseointegrative layer, which were obtained as a part of an ongoing retrieval program at the first author's institution (IRB approval 162/12). After examining the collected implants, three types of acetabular components with signs of coating failure were identified and included in this study—16 Biomet L-Cup (36 retrievals available, 1 case of coating failure with the implant still in situ), 3 Biomet ReCap (5 retrievals available), 1 Implantcast EcoFit (12 retrievals available). Additionally, 6 L-Cup, two ReCap and two EcoFit retrievals with undamaged TPS coatings were also included as reference samples of undamaged coatings (Table 1).

The first type of implant is made from Ti6Al4V alloy and features a peripheral threaded part with a smooth surface finish for improved primary stability (Fig. 1a-c). The central part was fitted with three screw holes and coated with TPS applied following grit blasting. The EcoFit cup was made from Ti<sub>6</sub>Al<sub>4</sub>V alloy with the whole outer surface treated by grit blasting and TPS application (Fig. 1d). The ReCap components are made from CoCrMo alloy and feature four pairs of peripheral fins for improved primary stability. In these implants, the outer surface was grit blasted and TPS coated with the exception of the inner part of each pair of fins and the fins themselves (Fig. 1e, f).

The implants were obtained during revision surgeries performed due to aseptic loosening, osteolysis, or severe polyethylene wear in 11 males and 9 females. The mean age at revision was 67.2 years (range 48-78), and the mean in vivo survival time was 9.7 years (range 5.1-14.2); data regarding BMI of patients at revision as well as their physical activity levels following implantation of total hip replacements were also collected (Table 1). UCLA score was used for activity evaluation as it is easy to apply and has good reliability (Ref 25). In 10 cases, samples of periprosthetic tissues were obtained for pathological examination; they underwent standard histologic processing (fixation in buffered formalin, dehydration in a series of ethanol solutions, clearing in xylene and embedding in paraffin blocks). Sections of these blocks were used to prepare microscopic slides stained using routine hematoxylin—eosin staining (Ref 26, 27). Small fragments of the debonded coating still attached to the acetabular bone were also obtained during some procedures (5 L-Cup fragments, 1 ReCap, and 1 EcoFit sample).

**Table 1** Clinical and demographic data of patients whose implants were included in this study

Number	Manufacturer	Implant model	Sample type	M/F	Age at revision	Service time (months)	Tissue fragments	Bone + coating fragments	BMI at revision	Max UCLA post-op	Metallographic sample
1	Biomet	L-cup	Retrieval—total debonding	Male	72	171	Yes	Yes	30,1	6	No
2	Biomet	L-cup	Retrieval—total debonding	Female	75	126	No	No	28,1	5	No
3	Biomet	L-cup	Retrieval—total debonding	Female	68	103	No	Yes	26,7	5	No
4	Biomet	L-cup	Retrieval—total debonding	Female	56	140	Yes	No	32,3	6	No
5	Biomet	L-cup	Retrieval—total debonding	Male	78	121	Yes	No	26,4	n.a.	No
6	Biomet	L-cup	Retrieval—partial debonding	Female	69	155	No	No	28,3	5	Yes
7	Biomet	L-cup	Retrieval—partial debonding	Male	58	165	Yes	No	29,8	6	Yes
8	Biomet	L-cup	Retrieval—partial debonding	Male	61	131	No	No	24,5	7	No
9	Biomet	L-cup	Retrieval—partial debonding	Female	74	125	Yes	No	28,6	5	Yes
10	Biomet	L-cup	Retrieval—partial debonding	Male	78	141	No	Yes	29,5	5	No
11	Biomet	L-cup	Retrieval—partial debonding	Male	72	121	No	No	30,4	4	No
12	Biomet	L-cup	Retrieval—partial debonding	Female	70	105	Yes	No	32,5	6	Yes
13	Biomet	L-cup	Retrieval—partial debonding	Female	69	117	No	No	35,2	5	No
14	Biomet	L-cup	Retrieval—partial debonding	Male	77	109	No	No	27,6	4	No
15	Biomet	L-cup	Retrieval—partial debonding	Male	72	126	Yes	No	32,5	5	No
16	Biomet	L-cup	Retrieval—partial debonding	Male	63	112	No	No	31,8	4	No
17	Biomet	ReCap	Retrieval—partial debonding	Male	48	49	No	No	29,2	7	Yes
18	Biomet	ReCap	Retrieval—partial debonding	Female	51	78	Yes	Yes	28,2	8	Yes
19	Biomet	ReCap	Retrieval—partial debonding	Female	61	63	Yes	No	25,7	7	No
20	Implantcast	Ecofit	Retrieval—partial debonding	Male	72	62	Yes	Yes	29,2	8	Yes
21	Biomet	L-cup control	Control	Female	76	118	Yes	No	30,2	5	Yes
22	Biomet	L-cup control	Control	Male	78	167	No	No	28,5	5	Yes
23	Biomet	L-cup control	Control	Female	72	177	No	No	31,8	6	No
24	Biomet	L-cup control	Control	Female	68	137	Yes	No	27,6	3	No
25	Biomet	L-cup control	Control	Female	81	161	No	No	26,3	5	Yes
26	Biomet	L-cup control	Control	Female	69	126	No	No	26,5	5	No
27	Biomet	L-cup liner revision	Radiographs only	Female	74	186	No	No	27,2	n.a.	No
28	Biomet	ReCap	Control	Male	57	39	No	No	29,5	7	Yes
29	Biomet	ReCap	Control	Male	36	28	No	No	27,2	8	Yes
30	Implantcast	Ecofit	Control	Female	72	76	No	No	27,5	6	Yes
31	Implantcast	Ecofit	Control	Female	81	103	No	No	26,8	6	Yes

M/F male/female, BMI body mass index, Max UCLA maximal postoperative UCLA activity score, n.a. non applicable—cases where data could not be obtained as the patients passed away due to reasons unrelated to the revision procedure

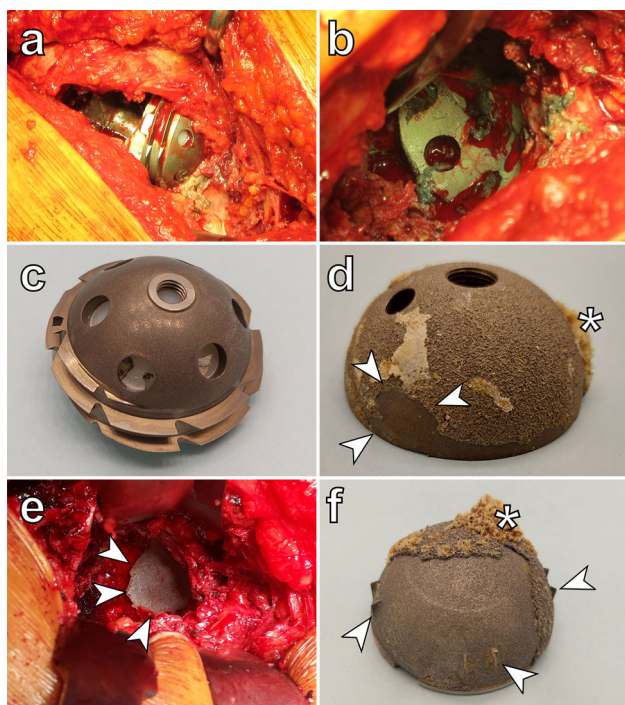


**Fig. 1** Implants included in the study: (a-c) Case 2: (a) Intraoperative view of a loose L-Cup component with a debonded TPS coating; (b) Fragments of the coating still attached to the acetabular bone; (c) A retrieved L-Cup component with a peripheral threaded part and six screw holes; (d) A retrieved EcoFit cup (case 20) with a partially debonded porous coating indicated by arrows; asterisk indicates area with bone still attached chosen for measurement of coating thickness (e, f) Failure of a ReCap component (case 17) (e) Intraoperative view of the debonded coating of the ReCap acetabular component; (f) A retrieved ReCap acetabular component with large fragments of coating missing; arrows indicate the antirotational fins present on this implant; asterisk indicates area with bone still attached chosen for measurement of coating thickness

After retrieval, the components were washed with a soft nylon brush and sterilized with ethylene oxide or disinfected by soaking in formaldehyde for 72 h. The samples were then visually inspected and examined using scanning electron microscopy (SEM; Philips XL-40, FEI InspectS) with x-ray energy dispersive spectroscopy (EDS; Apollo, Edax). SEM imaging and EDS analyses were performed at a 20 kV accelerating voltage, and backscattered electron images were obtained using an annular silicon detector. Next, selected samples (Table 1) with representative coating failure modes or areas where macroscopic fragments of bone (at least 4 mm in diameter) were still attached to the TPS layer were cut into smaller fragments using a low-speed diamond saw (Buehler Isomet). These fragments were used to prepare metallographic specimens for evaluation with optical and scanning microscopy, and fragments with bone attached were chosen for thickness measurements to minimize potential coating damage related to implant loosening or migration. To minimize

sectioning bias (cutting plane error), care was taken to orient the samples such that the resulting cross section was perpendicular to the outer surface of the cups. These samples were then used to measure coating thickness. In each sample, at least 20 uniformly distributed spots were selected over a distance of at least 3 mm. The thickness in these areas was measured perpendicular to the base metal using the measurement function of the SEM software. This data was analyzed using GraphPad Prism 10.2.3 software. Briefly, as the lack of normal distribution of results was confirmed using the Shapiro–Wilk test, data from implants with and without coating failure were compared using the Mann-Whitney test.

## Results

In this study, the primary location of debonding of the TPS coating was found to be at the coating-shell interface, with only two L-Cup components showing areas of cohesive failure. Visual inspection revealed two distinct morphologies of TPS coating debonding (Fig. 2a). In components where no migration occurred, the denuded cup parts showed a rough surface finish with grit blasting marks, and the corresponding surface of the debonded coating exhibited a rough surface as well. However, in implants that migrated *in vivo* due to loosening (L-Cup retrievals only), partial wear-induced smoothing and polishing of the grit blasted cup surface and the debonded coating fragments were observed (Fig. 2a). Multiple metallic third bodies were found embedded into the polyethylene liners in these cases (Fig. 2b). Total coating failure resulted in the polishing of the entire outer surface of the cups, while a mixture of both morphologies was observed in implants with partial TPS delamination and implant migration.

The outer surface of the TPS coating in implants with no migration displayed no signs of wear, and fragments of acetabular bone were still attached to it. In implants with partial failure and migration, certain areas of the coating remained undamaged and had bone fragments attached, while other areas showed signs of polishing. In two implants, areas with cohesive coating failure characterized by mostly rough surface with localized polishing were identified. (Fig. 2a)

These results were further confirmed by SEM analyses. Rough denuded areas not damaged by implant migration had well-defined borders with a cliff-like appearance on SEM micrographs (Fig. 3a, c, e). However, in some components, crevices were found between the debonded coating and the bulk material of the acetabular cup near the edges of the cups or screw holes (Fig. 3a, e). The surface of these denuded areas featured distinctive grit blasting marks and small alumina grains embedded into the cup material

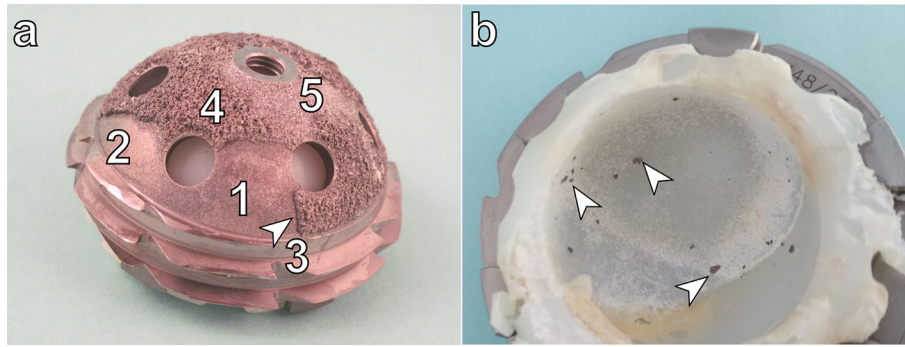


**Fig. 2** A L-Cup retrieval with various modes of coating failure present: (a) TPS layer debonding with rough (1) outer surface and areas of localized polishing (2). A crevice (3) visible at border (arrow)

of the intact coating (4); small areas of cohesive failure (5) near the polar region (b) the PE liner of this implant underwent severe wear, accelerated by the presence of metallic third bodies (arrows)

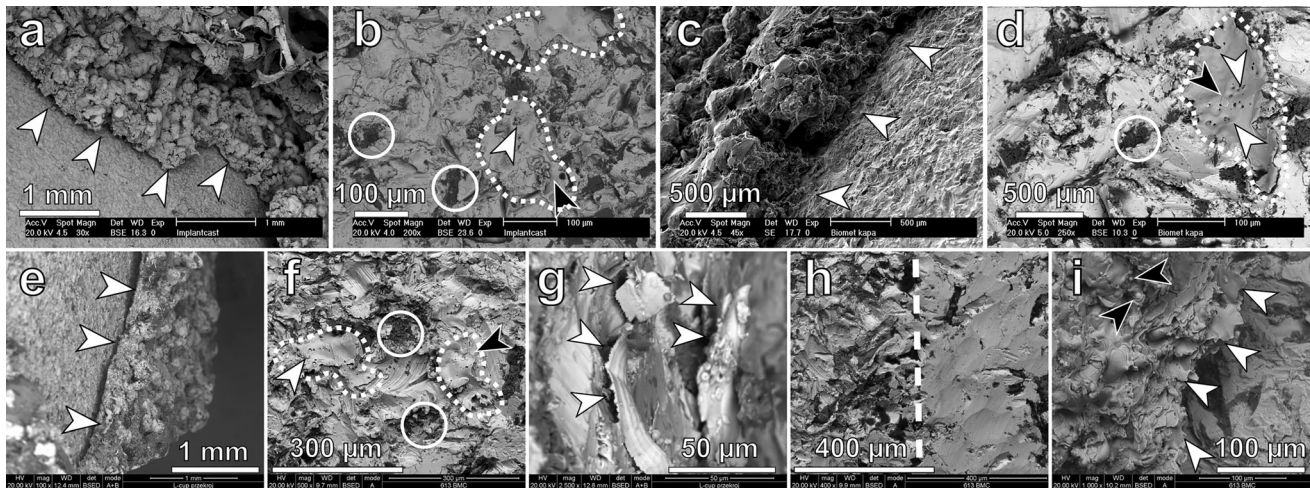


**Fig. 3** SEM examination of the retrieved components: (a) The cliff-like edge of coating failure in an EcoFit cup; arrows indicate a crevice beneath the still attached coating (corresponding to Fig. 1d—border indicated by arrows); (b) Denuded areas of the EcoFit cup (corresponding to fit 1d) : marks caused by grit blasting with embedded alumina particles (in circles); splashed splats (outlined with dotted lines) with voids (white arrows) and droplets (black arrows); (c) The cliff-like edge of coating failure in a ReCap component (corresponding to Fig. 1c); a small crevice marked by arrows; (d) Denuded part of the ReCap component (corresponding to Fig. 1c)—grit blasted surface with embedded alumina grains (in circles); a splashed splat (outlined by a dotted line) with voids (white arrows) and droplets (black arrow) is visible; (e) The edge of coating failure in an L-Cup component (corresponding to Fig. 2a; region marked as 3); arrows indicate a crevice beneath the debonded coating;

(f) Denuded area of an L-Cup implant (corresponding to Fig. 2a; region marked as 1)—grit blasted surface with alumina grains (in circles) embedded into the base material; splashed splats (outlined by dotted lines) with voids (white arrows) and droplets (black arrows); (g) Individual splats from an L-Cup component (corresponding to Fig. 2a; region marked as 1); arrows indicate peripheral detachment of these splats from the base material; (h) Fragment of an L-Cup retrieval (corresponding to Fig. 2a; region marked as 2) where wear-induced smoothing of the outer grit blasted surface due to implant migration is visible to the right of the dashed line; undamaged surface to the left; (i) Areas of cohesive failure in the L-Cup implant (corresponding to Fig. 2a; region marked as 5); splats (white arrows) do not contain voids; however, multiple droplets (black arrows) were present

(Fig. 3b, d, f). In all types of implants, these rough areas contained individual titanium alloy splats with an irregular shape. The splats contained small voids, and multiple small droplets and splashes were visible in their proximity (Fig. 3b, d, f), while their borders were often not attached to the base material (Fig. 3g). Parts of cups polished due to implant migration exhibited flattening of the grit blasting marks and removal of most alumina grains (Fig. 3h). Areas of cohesive failure also had well-defined cliff-like borders

and were characterized by the presence of multiple irregular splats with very few voids, however, a large number of droplets were present between them (Fig. 3i).

The adherent surface of the delaminated coating fragments was composed of titanium alloy splats with a comparable morphology and a small number of alumina grains pulled out from the cup's bulk material (Fig. 4a-c). Detached fragments of coatings corresponding to polished fragments of the L-Cup shells had a smooth surface with

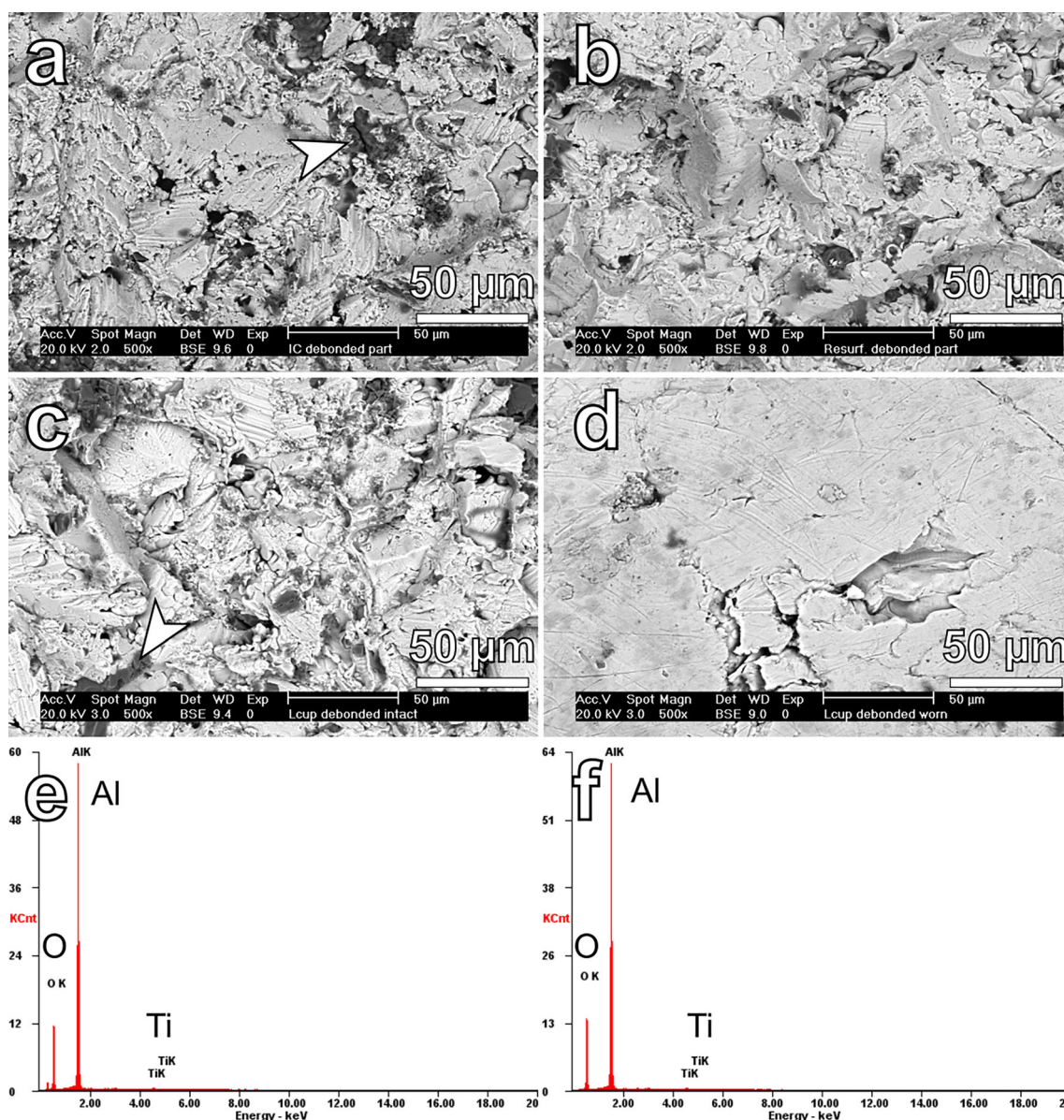


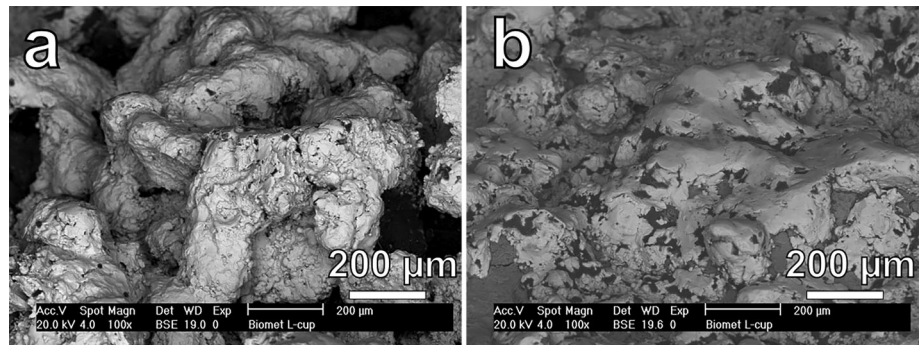
**Fig. 4** SEM analysis of debonded coating fragments—the side previously attached to the cups visible on all micrographs: (a) Coating from the EcoFit cup—splats with a small number of alumina grains visible arrow indicates a grain evaluated using EDS (Fig. 4e); (b) Coating detached from the ReCap component; multiple splats, droplets and small alumina grains; (c) Coating fragment detached from an L-Cup component consisting of splats, droplets and alumina grains; arrow indicates a grain analyzed using EDS (Fig. 4f) (d) A

thin boundaries between the splats forming the TPS coating visible (Fig. 4d).

In controls and retrievals that did not migrate the outer surface of the TPS coating consisted of splats and droplets forming a porous macrostructure overgrown by bone (Fig. 5a). Implant migration also affected the appearance of the outer coating surface resulting in localized polishing

observed in samples with partial debonding and some controls (Fig 5b). Metallographic cross sections revealed a clear demarcation between the bulk cup material and the TPS coating in all components, including the controls. The splats in the TPS exhibited interlocking with the rough outer surface of the implant and alumina grains, with no metallurgical bonding occurring at the interface (Fig. 6a-c). Borders

**Fig. 5** SEM analysis of the outer surface of coating from L-Cup retrievals (a) Typical appearance of undamaged coating—multiple splats and droplets forming a porous structure (corresponding to Fig. 2a; region marked as 4); (b) flattening of the porous structure due to wear and polishing related to implant migration (sample 21—control)



between splats forming consecutive layers of the coating were typically less distinct, and metallurgical bonding was commonly observed. Near areas where coating failure occurred, the demarcation between the TPS layer and cup material extended into a gradually widening gap, which was observed in both the cliff-like borders and the areas where a crevice was formed (Fig. 6a-c).

In order to determine if coating thickness, structure, and chemical composition differed between implants with and without debonding, metallographic sections in areas with bone attached to retrieved components were evaluated. In the case of L-Cup implants (Fig. 7a-d), there was no statistically significant difference between the thickness of the TPS layer in implants with (mean 480.72 µm; range 181-973 µm) and without (mean 516.28 µm; range 147-1102 µm) coating failure. On the ReCap samples (Fig. 7e-h) comparable TPS layer thickness was found in implants without debonding where (mean 527.73 µm; range 180-1066 µm), and in samples with debonding (mean 542.53 µm; range 139-1386 µm). There was also no statistically significant difference between the EcoFit samples (Fig. 7 i-l); mean coating thickness in the implant with debonded coating was 416.32 µm (range 91-891 µm), while in controls, it was 394.87 µm (range 110-1281 µm). In all types of implants, there were no noticeable differences in coating structure between implants with and without debonding. EDS analyses did not demonstrate the presence of any contamination in any of the samples.

Data from serial radiographs available for some patients suggest that the debonding process may be initiated in the lower part of the acetabulum corresponding to zone 3, according to DeLee and Charnley (Fig. 8). Remarkably, one patient with coating debonding and liner wear gave consent to undergo a liner exchange only, and after this procedure, the acetabulum has (as of writing) been asymptomatic for the last 5 years (Fig. 8a-c). In a different patient, asymptomatic debonding was confirmed as early as 3 years before any symptoms were present and 5 years before the implant was revised due to migration and polyethylene wear (Fig. 8d-f)

In other patients where serial images were not available, the evaluation of radiographs was challenging (Fig. 9). In some cases where no apparent coating delamination was observed on preoperative x-rays (Fig. 9a-d), the retrievals had partial debonding with the rough grit-blasted surface of the substrate material exposed, suggesting that the failure occurred during implant removal. In one case of partial failure (Fig. 9e), a small debonded fragment was visible on x-rays, and a larger debonding area with mixed (rough and smoothed) surface morphology was observed on the retrieval. Interestingly, in two cases of partial failure, debonded coating fragments could not be detected on standard AP prone radiographs but were visible on either an axial view (Fig. 9f, g) and in one case on a standing AP view (Fig. 9i, j). This was most likely a result of a slight change in the cup's position while these radiographs were taken; also in both cases debonding with abrasion induced surface polishing was observed. Still, in all patients where at least some signs of partial coating debonding were observed, they occurred in DeLee and Charnley zone 3.

Pathological examination of periprosthetic tissues revealed distinct morphological differences depending on the failure mechanism; however, samples were only available for some of the patients with MoP bearings. The interfacial membrane obtained from controls and cases where implant migration did not occur exhibited a white-yellowish color and contained polyethylene debris in cases of liner wear and small amounts of metallic debris when component loosening occurred (Fig. 10a-d). In contrast, samples from cases with total or partial debonding and implant migration displayed a dark color and contained a significant number of macrophages loaded with metallic and polyethylene debris (Fig. 10e-f).

## Discussion

Plasma sprayed coatings have been widely used in joint replacements for decades, and due to strict testing protocols and regulations, they are considered reliable (Ref 2, 3). Although several reports regarding their failure exist, the

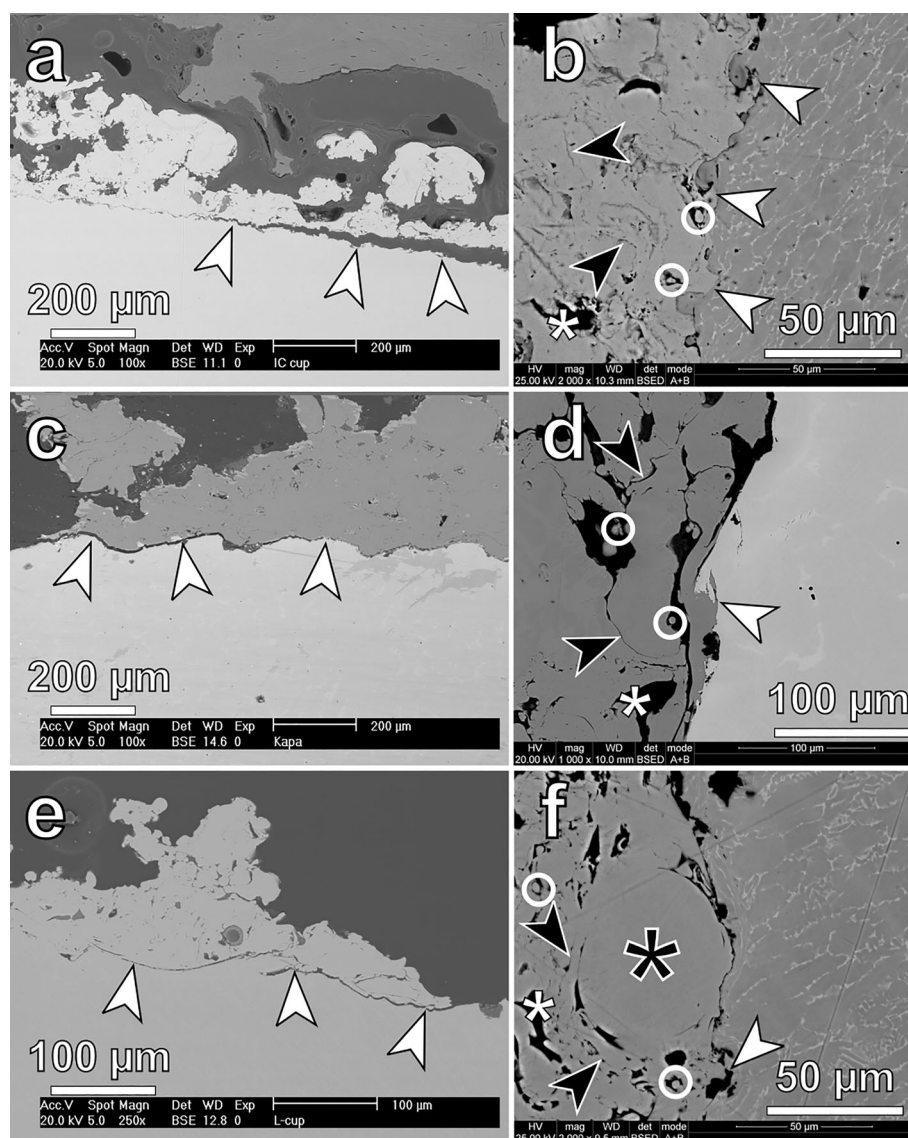


**Fig. 6** SEM analysis of metallographic cross sections of all types of components (a) delamination in the EcoFit cup (corresponding to Fig. 1d): arrows indicate a gap between the coating (upper part of the micrograph) and the base material that gradually extends to the right. (b) cross section of the coating—base material interface in a EcoFit control sample (case 29) demonstrating mechanical interlocking of the coating (white arrows), thin borders between splats (black arrows) and presence of voids (white asterisks) and droplets (white circles) in the TPS layer. (c) coating failure in a ReCap implant (corresponding to Fig. 1f): arrows indicate a gap between the coating (upper part of the micrograph) and the CoCrMo base material. (d) cross section of the interface of coating—base material of a ReCap control sample (case 28) demonstrating mechanical interlocking of the coating and

base material (white arrow), borders between splats (black arrows) and presence of voids (white asterisks) and droplets (white circles) in the TPS layer. (e) Coating failure in an L-Cup implant (corresponding to figure 2a; border of the coating in region marked as 1): arrows indicate a gradually widening gap between the TPS layer (upper part of the micrograph) and the base material. (f) cross section of the interface of coating—base material of a L-Cup control sample (case 21) demonstrating mechanical interlocking of the coating and the substrate material (white arrow), borders between splats (black arrows) and presence of voids (white asterisks) and droplets (white circles) in the TPS layer; an unmelted titanium particle visible in the center (black asterisk)

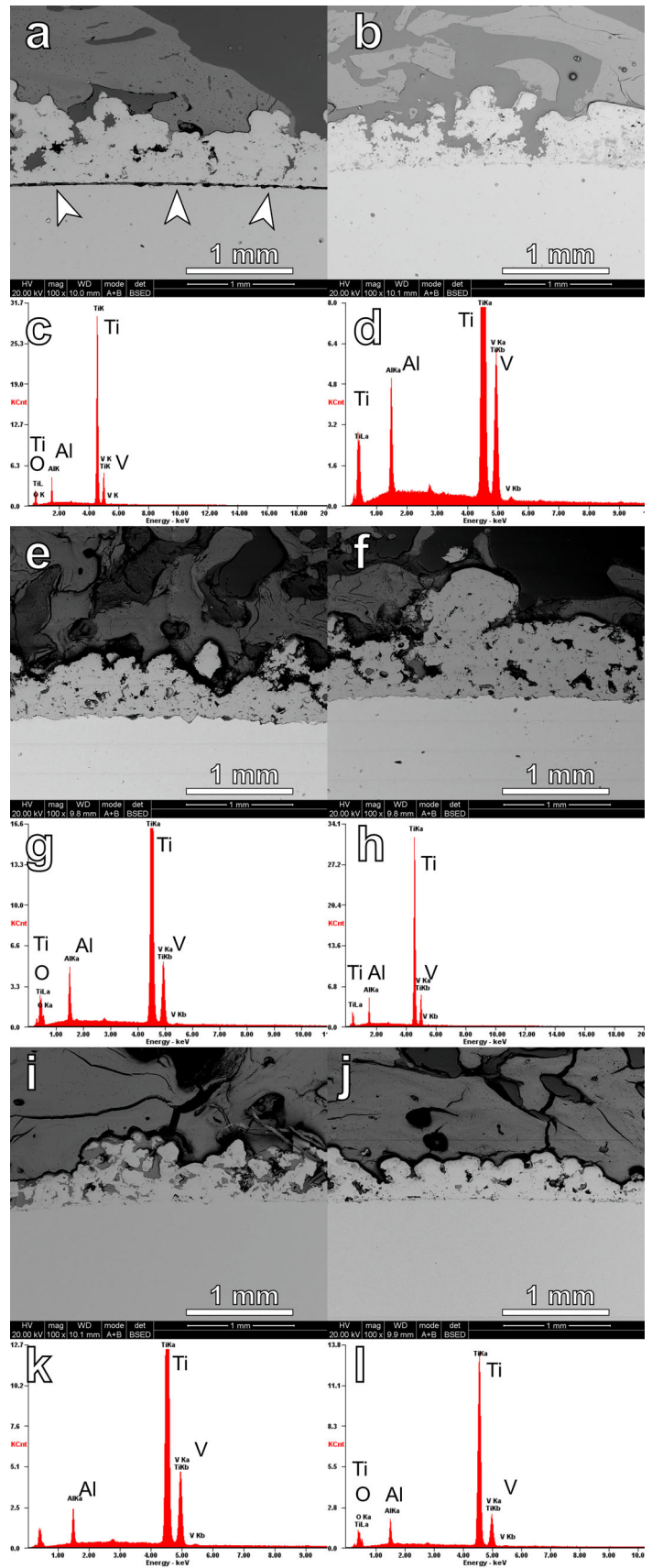
underlying mechanisms remain largely unexplored (Ref 19, 20). This study offers insight into the issue by demonstrating that debonding of such coatings may occur due to fatigue fracture at the implant-coating interface.

Coating failure in joint arthroplasty is not solely limited to ingrowth layers made from plasma-sprayed titanium

particles. Previous studies, mostly regarding acetabular components, have shown shedding of sintered beads and fatigue of wire-mesh coatings due to inadequate bonding strength (Ref 13-15). Debonding of hydroxyapatite coatings has also been reported in both acetabular and femoral components, with suggestions that hydroxyapatite may



**Fig. 7** Thickness evaluation of coating in implants with and without coating failure: (a) Cross section of an L-Cup implant with partial coating failure (Case 12); arrows indicate the area where debonding occurred (b) L-Cup control sample (Case 22) cross section (c) EDS analysis of a  $200 \times 200 \mu\text{m}$  coating fragment from Fig. 7a (d) EDS analysis of a  $200 \times 200 \mu\text{m}$  coating fragment from Figure 7b (e) Cross section of a ReCap implant (Case 17) with partial coating failure (f) ReCap control sample (Case 28) cross section (g) EDS analysis of a  $200 \times 200 \mu\text{m}$  coating fragment from Fig. 7e (h) EDS analysis of a  $200 \times 200 \mu\text{m}$  coating fragment from Fig. 7f (i) Cross section of an EcoFit implant (Case 20) with partial coating failure (j) EcoFit control sample (Case 31) cross section (k) EDS analysis of a  $200 \times 200 \mu\text{m}$  coating fragment from Figure 7i (l) EDS analysis of a  $200 \times 200 \mu\text{m}$  coating fragment from Fig. 7j



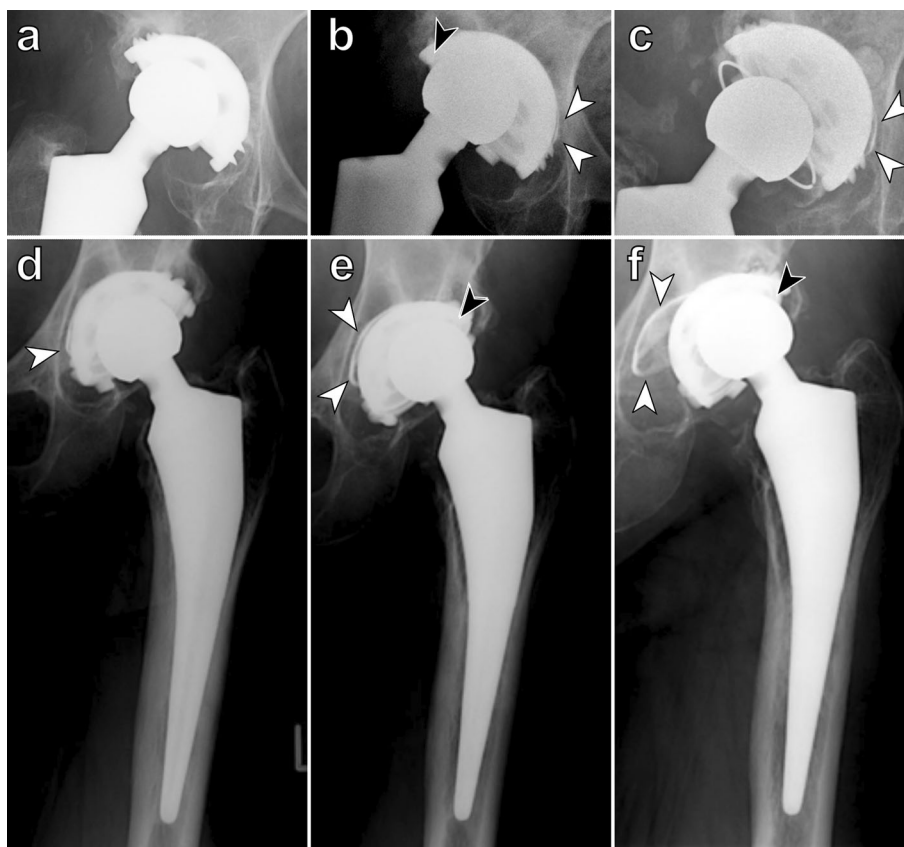


**Fig. 8** Serial radiographs demonstrating progression of coating debonding in two hips (a–c—case 27; d–f—case 2) with L-Cup components; (a) routine check-up radiograph from 2009—no signs of coating damage; (b) radiograph from 2018 prior to revision due to PE liner wear (black arrow), coating debonding in Gruen zone III visible (white arrows); the patient gave consent only for liner exchange. (c) radiograph from 2023—no major implant migration; coating debonding indicated by white arrows. (d) routine check-up radiograph

from 2010—initial coating debonding (white arrow) in an asymptomatic patient; (e) subsequent radiograph from 2013—the patient developed mild pain and was initially qualified for revision due to liner wear (black arrow); white arrows indicate debonded coating. (f) radiograph from 2015, shortly before the revision; cup migration exposed the debonded coating (white arrow); severe liner wear (black arrow)

detach from the implant after some time as it becomes resorbed in vivo (Ref 16, 28). Several factors, such as the chemical composition and texture of the underlying substrate, appear to play a significant role in this process (Ref 6).

Although data on TPS coating failures comes mostly from case studies, evidence suggests that these failures may not be isolated incidents. For example, Robinson et al. reported a 3.5% incidence of debonded coating in a cohort of 371 Corin Cormet hip resurfacing implants with a minimum follow-up of 10 years (Ref 11). While no retrieval analysis was conducted in that study, other reports have described cases of TPS failure in similar implants, including those by Ray et al. and Jacobs et al (Ref 20, 29). In the latter study, one retrieved implant was subjected to independent mechanical analysis, which revealed no manufacturing issues but did not provide conclusive evidence on the failure mechanisms (Ref 20).

Debonding of TPS coatings has also been reported in threaded acetabular components, with several case reports available (Ref 17–19). While one such component was subjected to retrieval analysis, the mechanism of failure could not be explained due to damage caused by loosening (Ref 19). Delpont et al. also reported TPS debonding in a Biomet ReCap resurfacing cup, with the failure occurring near the polar part of the cup (Ref 21).

TPS coatings can bond to base materials through physical, metallurgical, and mechanical mechanisms (Ref 30). As pointed out by Meghwal et al, the effectiveness of plasma-sprayed coating depends on the quality of the substrate/coating interface adhesion bond and on the cohesion of buildup layers. (Ref 31) In contemporary medical implants, including those investigated in this study bonding of the TPS layer is enhanced by grit blasting. This process ensures mechanical bonding as molten particles spread out to fill any grooves and pits; it is chosen due to its

**Fig. 9** Radiographs from patients where serial images were not available: (a, b) Case 10—L-Cup implant; partial debonding: (a) Radiograph from 2014—no apparent debonding (b) Radiograph from 2017—no apparent debonding (c-d) Case 17—ReCap implant; partial debonding: (c) Radiograph from 2019—no TPS failure (d) Radiograph from 2021—no coating damage (e) Case 14—L-Cup implant, partial coating failure; arrow indicates a small debonded coating fragment. (f-h) Case 12—L-Cup implant; partial failure: (f) Preoperative prone AP radiograph taken in 2020—no signs of coating damage (g) Axial radiograph taken the same day—arrow indicates the area where coating debonding became apparent (h) Enlarged part of Figure 9 g—arrows indicate the debonded fragment (I, j) Case 16—L-Cup implant: (i) Radiograph from 2018—no apparent coating damage on prone AP view (j) Standing AP radiograph taken two weeks later with debonding visible—arrows indicate the debonded fragment. The patient did not report any falls or changes in symptoms suggesting debonding between the radiographs

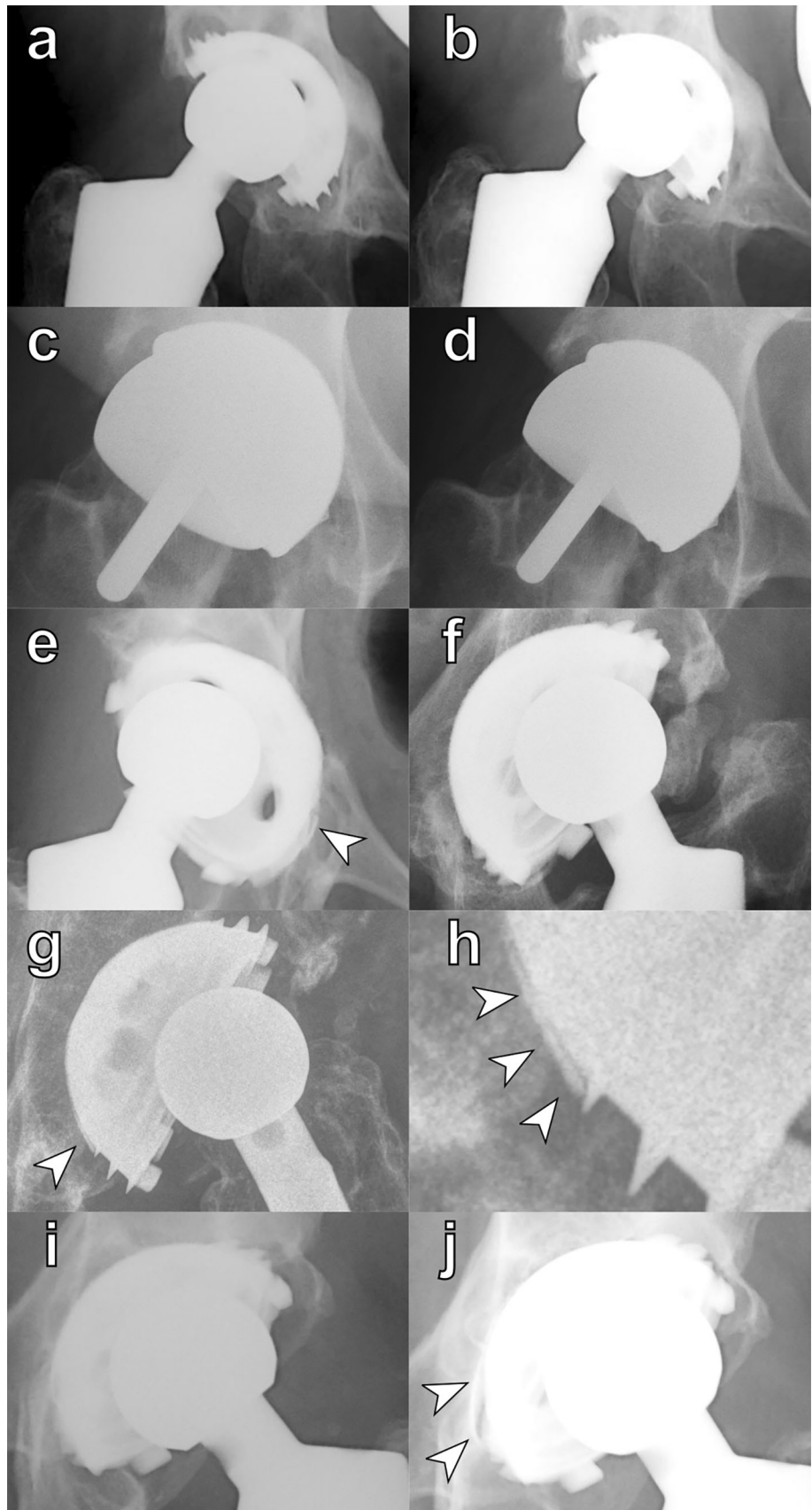
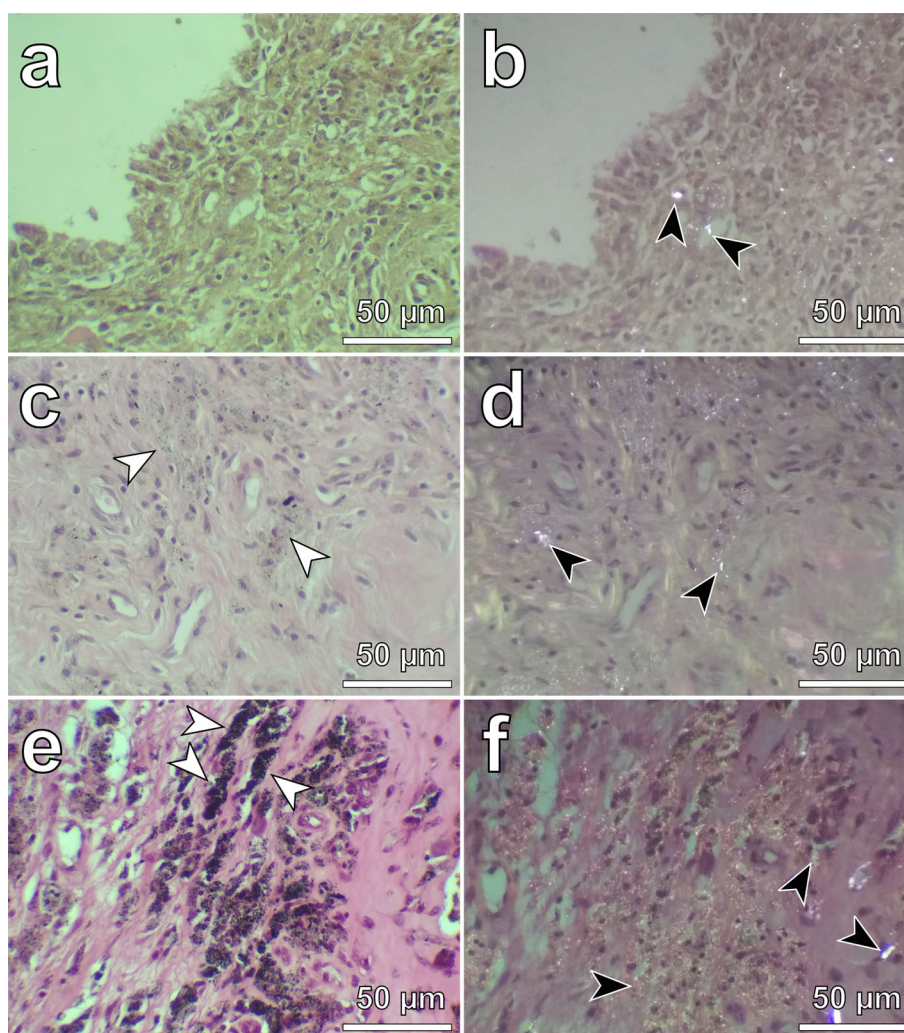


**Fig. 10** Paired microscopic slides of periprosthetic tissues from patients with L-Cup failures; images on the left were taken using standard conditions, while those on the right were taken using polarized light to visualize polyethylene debris. (a) Conventional image of a control case—L-Cup implant loosening due to PE wear; typical morphology of an interfacial membrane associated with aseptic loosening. (b) The same part of the slide under polarized light; black arrows indicate polyethylene debris. (c) Periprosthetic tissue from a patient with partial debonding and no migration; macrophages with small amounts of metallic debris marked by white arrows. (d) The same tissue fragment under polarized light; black arrows indicate polyethylene debris. (e) Fragment of periprosthetic tissue from a patient with coating debonding and implant migration; white arrows indicate macrophages loaded with metallic debris. (f) The same fragment under polarized light; polyethylene debris indicated by black arrows



cost-effectiveness and proven clinical record (Ref 30, 32, 33).

SEM studies of retrieved components with and without coating failure revealed that mechanical bonding was the predominant mechanism of coating adhesion in all samples. On metallographic samples, a clear demarcation was observed at the interface between the coating and substrate material with embedded alumina grains, while the borders between individual splats forming the coating were less distinct and some metallurgical bonding most likely occurred between them (Ref 30). Additionally examination cross sections and the denuded areas of implants with partial debonding revealed the presence of irregular splats with voids and multiple small droplets. Studies have shown that such splats are formed when there is a high temperature gradient between the substrate material and molten splats and they typically have point-like bonding with the substrate material (Ref 32-36). Voids are believed to form due to gas or moisture evaporation from the substrate

material's surface, while droplets form during the impact of splats with the substrate material (Ref 32, 34, 35, 37).

These microscopic features suggest that fatigue-related coating failures in the examined retrievals were associated with increased residual stress. It can arise due to the thermal and mechanical interactions during the coating process and has a significant impact on bonding strength (Ref 38). The defects observed in splats deposited directly on the substrate material can induce various failure mechanisms in plasma-sprayed coatings, including interfacial debonding, cracking, and spalling (Ref 9, 22, 31). Furthermore, residual stresses can change over time due to various factors such as mechanical loading, or exposure to environmental conditions leading to its relaxation or redistribution (Ref 9, 31). Stress relaxation can potentially lead to the development of new cracks or the propagation of existing ones, intersplat sliding and plastic deformation of splats, affecting the coating's bonding and performance (Ref 22, 23, 38). Most likely a combination of these failure mechanisms was responsible for coating delamination

observed in this study, and it is not possible to determine which of them played the most important role. Still, based in the crevices' location and propagation pattern it can be assumed, that debonding was initiated at the coating's border near the outer edge of the cup or fragments of the implants that were not coated, such as screw holes or antirotational fins. Such borders are obtained by masking fragments of the implant before plasma spraying, and precracks are formed in these regions (Ref 22). Interestingly, Otsu et al. demonstrated that debonding of hydroxyapatite coatings of acetabular components caused by cyclic loading occurred in the lower parts of the cups (Ref 5-8). This is consistent with radiographic data for cases with asymptomatic debonding, where failure was observed in the lower part of the acetabular components near their rim, corresponding to Gruen zone III on radiographs.

Robinson et al. pointed out that a steep inclination angle of acetabular components might be a risk factor for coating failure, while Otsuka et al. suggested that the anteversion angle of the component could play a significant role in coating adhesion (Ref 5, 11). However, these parameters did not seem to play a critical role in this study, as most components had inclination angles within the recommended values, and data on component anteversion were not available. It is important to note that this mechanism may not account for all the failures in this series, as some fragments may have debonded during implant removal, and examination of components that migrated in vivo is inconclusive due to damage from aseptic loosening. Some design parameters might have also contributed to the failures observed. Most of the retrievals were L-Cup implants, featuring a partially threaded, smooth part and multiple screw holes. As a result, only a small fraction of the cup is covered by the TPS layer, which may increase interfacial stress during loading and contribute to coating failure (Ref 19).

Several methods have been explored to improve coating adhesion. Some studies have shown that fine-tuning TPS parameters results in the formation of round splats with increased contact area with the substrate material and stronger bonding (Ref 32, 34, 35, 39-41). However, in the case of medical implants, this may not be desirable, as coatings formed by such splats are characterized by low porosity, which would not promote bony ingrowth. Other techniques, such as hot isostatic pressing (HIP), have also been applied. Still, as demonstrated by Robinson et al., this did not prevent coating failures in the Corin Cornet implants (Ref 11, 20, 42). It could be hypothesized that a "gradient" or a two-stage process could be used to manufacture improved coatings, consisting of a "bonding" layer of round splats below a porous "osseointegrative" layer. Although such coatings are characterized by reduced residual stress (Ref 23), it remains uncertain whether this

process would indeed improve long-term coating adhesion, and its economic feasibility is questionable. Several techniques have been designed for reducing the residual stress of TPS layers, such as inert gas-shrouded or vacuum plasma spraying (VPS). Although such coatings have favorable mechanical (reduced residual stress), chemical (reduced interactions with oxygen and nitrogen minimizing splat brittleness) and biological properties (high porosity), their manufacturing cost is higher, and data on long-term clinical performance is not yet available (Ref 31, 43).

Although the authors believe that the coating debonding observed in this study was mechanical in nature and resulted from the mechanism described above, other possibilities should be considered as well (Ref 6, 7, 9, 44). Metallographic examination demonstrated that coating thickness and structure were comparable in samples with and without debonding. Although such data is not available for implants with total debonding, it could be assumed that the TPS process resulted in consistent layers in all examined cases and failures were not related to differences in their thickness (Ref 9, 23, 23, 38). Another possibility could be "overloading" of the coating by patients with excessive BMI or engaging in high-impact physical activity (Ref 5-7). However, in this study, there were no patients with morbid BMI or very high physical activity in either group. Moreover, physical activity and BMI were comparable between cases of coating failure and controls. It could therefore be concluded that patient-related factors did not play an important role. Another potential failure mechanism could be chemically induced debonding (Ref 8, 44). All TPS layers described in this study had identical chemical compositions, so we cannot fully verify this hypothesis. However, it should be noted that the EcoFit and L-Cup implants had the same titanium alloy used as a base material, while the ReCap components were made from a CoCrMo alloy. Nonetheless, SEM studies did not demonstrate signs of corrosion within the coating or at the interface, and EDS examination confirmed a consistent chemical composition of both coating and substrate materials. Still, we cannot rule out that some minor contamination could have been involved at some point of the failure.

It should be noted that the findings of this study have important clinical implications. Historically, coating failure has been viewed as an incidental failure mode; however, this study, along with Robinson et al.'s data, suggests that the incidence of TPS debonding may be underestimated (Ref 11). This is consistent with our findings as it was challenging to find radiographic signs of debonding in several of our patients as failures can occur without symptoms and progress over many years, resulting in the release of metallic debris and accelerated polyethylene wear (Ref 19). This, in turn, leads to osteolysis and implant

loosening, thereby highlighting the need for regular radiographic check-ups of asymptomatic THRs, even many years after implantation. Given the widespread use of these coatings in clinical settings, surgeons must be aware of this issue.

The authors believe that TPS debonding detected on radiographs should be considered as a relative indication for implant revision, since it tends to progress over time, as evidenced by serial radiographs. However, in instances where the patient or surgeon decides against undergoing a revision surgery, regular radiographic check-ups should be performed to monitor the situation closely.

Our study is limited in several ways, predominantly due to the fact that it includes a small number of samples mostly from one manufacturer, thus our findings may not apply to other types of implants with porous coatings. As in all retrieval studies, our samples do not represent well-functioning implants, so we are unable to determine if such a failure mode should be expected in other acetabular cups of this type. The cause of failure in some cases may have been related to patient factors, such as obesity or high activity levels, rather than implant-related issues. Finally, while SEM analysis is a useful tool for evaluating coating adhesion and failure mechanisms, it cannot provide information on the *in vivo* conditions that contributed to implant failure. EDS analyses used to determine the chemical composition of the coating have a limited precision and are insufficient to detect small scale contaminations. Finally, thickness measurements employed in this study have a limited precision as a limited number of samples were available.

## Conclusions

This study presented a series of acetabular components that experienced debonding of the porous coating during long term *in vivo* use. Retrospective analysis of retrievals suggests that these failures resulted from fatigue mechanisms, as demonstrated in previous laboratory studies. As failures were likely associated with suboptimal plasma spraying process parameters, thermal spray researchers should consider further development strategy in this field. This study also highlights the importance of more rigorous pre-clinical testing protocols in the development of future implants. New designs of acetabular components should avoid features that are not coated by the TPS layer, as this reduces the overall coated area while potentially increasing the number of failure initiation sites.

Although only a few similar failures have been reported thus far, it is important for surgeons to be aware of this issue, as other cases may emerge during long-term follow-up. The fact that some patients were asymptomatic

emphasizes the importance of regular radiographic assessments even many years after the primary procedure. In cases when such failure is suspected, it is of critical importance to review serial radiographs taken in various positions with and without weight-bearing as early failures is likely to be missed based on evaluation of a single radiograph. Although certain parameters associated with implant positioning have been proposed as potential risk factors for coating failure, data from this study did not support these claims.

In conclusion, it is essential to explore methods for enhancing coating adhesion while preserving desirable characteristics such as porosity, which promotes bony ingrowth. Several techniques may offer potential solutions, but their feasibility and effectiveness in medical implants must be thoroughly evaluated.

**Funding** This research did not receive any specific grant from funding agencies in the public, commercial, or not-for-profit sectors.

**Open Access** This article is licensed under a Creative Commons Attribution 4.0 International License, which permits use, sharing, adaptation, distribution and reproduction in any medium or format, as long as you give appropriate credit to the original author(s) and the source, provide a link to the Creative Commons licence, and indicate if changes were made. The images or other third party material in this article are included in the article's Creative Commons licence, unless indicated otherwise in a credit line to the material. If material is not included in the article's Creative Commons licence and your intended use is not permitted by statutory regulation or exceeds the permitted use, you will need to obtain permission directly from the copyright holder. To view a copy of this licence, visit <http://creativecommons.org/licenses/by/4.0/>.

## References

1. E. Swarts, T.A. Bucher, M. Phillips, and F.H.X. Yap, Does the Ingrowth Surface Make a Difference? A Retrieval Study of 423 Cementless Acetabular Components, *J. Arthroplasty*, 2015, **30**(4), p 706-712.
2. A. Palomäki, M. Hemmilä, M. Matilainen, A. Eskelinen, J. Haapakoski, A.-P. Puhto, J. Kettunen, K. Pamiilo, M. Manninen, A. Vasara, and K.T. Mäkelä, No Difference in Implant Survival Between 28-Mm M2a RingLoc Metal-on-Metal and Metal-on-Polyethylene Total Hip Arthroplasty: Results From the Finnish Arthroplasty Register, *Acta Orthop.*, 2022, **93**, p 854-858.
3. A. Palomäki, M. Hemmilä, I. Laaksonen, M. Matilainen, A. Eskelinen, J. Haapakoski, A.-P. Puhto, J. Kettunen, M. Manninen, and K.T. Mäkelä, Implant Survival of 6080 Tritanium Cups in Primary Total Hip Arthroplasty: Data From the Finnish Arthroplasty Register From 2009 to 2017, *J. Bone Jt. Surg.*, 2020, **102**(13), p 1177-1185.
4. K. Valancius, K. Søballe, P.T. Nielsen, and M.B. Laursen, No Superior Performance of Hydroxyapatite-Coated Acetabular Cups Over Porous-Coated Cups: An 8 Year Follow-up of 81 Patients From a Previously Reported Controlled Trial, *Acta Orthop.*, 2013, **84**(6), p 544-548.

5. Y. Otsuka, K. Kagaya, and Y. Miyashita, Effect of Delamination of Plasma Sprayed Hydroxyapatite Coating on Loosening Behaviors of Acetabular Cups Subjected to Cyclic Loading, *Eng. Fail. Anal.*, 2021, **127**, p 105548.
6. Y. Otsuka, D. Kojima, and Y. Mutoh, Prediction of Cyclic Delamination Lives of Plasma-Sprayed Hydroxyapatite Coating on Ti-6Al-4V Substrates with Considering Wear and Dissolutions, *J. Mech. Behav. Biomed. Mater.*, 2016, **64**, p 113-124.
7. Y. Otsuka, K. Kagaya, Y. Hakozaiki, Y. Miyashita, and Y. Mutoh, Effect of Interface Damage on Loosening Behavior of Acetabular Cup Subjected to Cyclic Loading, *Mater. Sci. Forum*, 2018, **941**, p 1841-1845.
8. M. Nagentrau, A.L. Mohd Tobi, S. Jamian, Y. Otsuka, and R. Hussin, Delamination-Fretting Wear Failure Evaluation at HAP-Ti-6Al-4V Interface of Uncemented Artificial Hip Implant, *J. Mech. Behav. Biomed. Mater.*, 2021, **122**, p 104657.
9. J.G. Odhiambo, W. Li, Y. Zhao, and C. Li, Porosity and its Significance in Plasma-Sprayed Coatings, *Coatings*, 2019, **9**(7), p 460.
10. A. Kienle, N. Graf, and H.-J. Wilke, Does Impaction of Titanium-Coated Interbody Fusion Cages into the Disc Space Cause Wear Debris or Delamination?, *Spine J.*, 2016, **16**(2), p 235-242.
11. E. Robinson, D. Gaillard-Campbell, and T.P. Gross, Acetabular Debonding: An Investigation of Porous Coating Delamination in Hip Resurfacing Arthroplasty, *Adv. Orthop.*, 2018, **2018**, p 1-10.
12. "SO 13179-1:2021 Implants for Surgery. Coatings on Metallic Surgical Implants Plasma-Sprayed Coatings Derived from Titanium or Titanium-6 Aluminum-4 Vanadium Alloy Powders, (2021)
13. A.R. Hsu, Z. Vaughn, and J.I. Huddleston, Early Catastrophic Failure of a Porous-Coated Acetabular Cup Due to Bead Shedding. A Case Report, *HIP Int.*, 2009, **19**(4), p 392-395.
14. D.J. Mayman, A.G. Della Valle, E. Lambert, J. Anderson, T. Wright, B. Nestor, T.P. Sculco, and E.A. Salvati, Late Fiber Metal Shedding of the First and Second-Generation Harris Galante Acetabular Component. A Report of 5 Cases, *J. Arthroplasty*, 2007, **22**(4), p 624-629.
15. G. Slullitel, A.G. Della Valle, M. Buttaro, and F. Piccaluga, Early Bead Shedding of the Vitalock Acetabular Cup—a Report on 7 Cases, *Acta Orthop. Scand.*, 2003, **74**(6), p 658-660.
16. M.A. Buttaro, J.I. Oñativia, P.A. Slullitel, M. Andreoli, F. Comba, G. Zanotti, and F. Piccaluga, Metaphyseal Debonding of the Corail Collarless Cementless Stem: Report of 18 Cases and Case-Control Study, *Bone Jt. J.*, 2017, **99-B**(11), p 1435-1441.
17. T.J.S. Puolakka, K.J.J. Pajamäki, P.O. Pulkkinen, and J.K. Nevalainen, Poor Survival of Cementless Biomet® Total Hip: A Report on 1047 Hips From the Finnish Arthroplasty Register, *Acta Orthop. Scand.*, 1999, **70**(5), p 425-429.
18. K. Barbaric Starcevic, G. Bicanic, S. Dokuzovic, D. Starcevic, and D. Delimar, Revision of Acetabular Component with a Debonded Porous Coating in an Elderly Patient, *Geriatrics*, 2020, **5**(4), p 73.
19. Ł Łapaj, J. Markuszewski, T. Rybak, and M. Wierusz-Kozłowska, Debonding of Porous Coating of a Threaded Acetabular Component: Retrieval Analysis, *J. Mech. Behav. Biomed. Mater.*, 2013, **17**, p 107-111.
20. M.A. Jacobs, T. Bhargava, J.M. Lathroum, and M.W. Hungerford, Debonding of the Acetabular Porous Coating in Hip Resurfacing Arthroplasty: A Report of Two Cases, *J. Bone Jt. Surg.-Am.*, 2009, **91**(4), p 961-964.
21. H.P. Delpont, B.V. Backle, and J.D. Scheppe, Debonding of the Acetabular Porous Coating in Hip Resurfacing Arthroplasty: A Case Report, *Acta Orthop. Belgica*, 2011, **77**, p 125-127.
22. T.W. Clyne and S.C. Gill, Residual Stresses in Thermal Spray Coatings and Their Effect on Interfacial Adhesion: A Review of Recent Work, *J. Therm. Spray Technol.*, 1996, **5**(4), p 401-418.
23. C.Y. Ning, Y.J. Wang, X.F. Chen, J.D. Ye, G. Wu, N.R. Zhao, K. Wei, L. Ren, and H.G. Liu, Research on Residual Stress and Surface Morphology of Bio-Functionally Gradient HA-ZrO<sub>2</sub>-Ti Coatings, *Key Eng. Mater.*, 2007, **330-332**, p 1301-1304.
24. E. Swarts, A.M. Kop, and M. Phillips, What are the Predictors for Bead Shedding in Porous-Coated Hip and Knee Arthroplasties?, *J. Arthroplasty*, 2012, **27**(10), p 1789-1795.
25. F.D. Naal, F.M. Impellizzeri, and M. Leunig, Which is the Best Activity Rating Scale for Patients Undergoing Total Joint Arthroplasty?, *Clin. Orthop.*, 2009, **467**(4), p 958-965.
26. R.D. Cardiff, C.H. Miller, and R.J. Munn, Manual Hematoxylin and Eosin Staining of Mouse Tissue Sections, *Cold Spring Harb Protoc*, 2014, **2014**(6), p p pdb.prot073411.
27. C.E. Day Ed., *Histopathology: Methods and Protocols*, (New York, NY), Springer, New York, 2014 <https://doi.org/10.1007/978-1-4939-1050-2>
28. K.-A. Lai, W.-J. Shen, C.-H. Chen, C.-Y. Yang, W.-P. Hu, and G.-L. Chang, Failure of Hydroxyapatite-Coated Acetabular Cups: Ten-Year Follow-up Of 85 Landos Atoll Arthroplasties, *J. Bone Joint Surg. Br.*, 2002, **84-B**(5), p 641-646.
29. R. Ray, E.B. Goudie, and P. Gaston, Debonding of the Acetabular Porous Coating of a Hip Resurfacing Arthroplasty: A Case Report, *HIP Int.*, 2012, **22**(2), p 230-232.
30. Y.Z. Yang, J.M. Tian, J.T. Tian, Z.Q. Chen, X.J. Deng, and D.H. Zhang, Preparation of Graded Porous Titanium Coatings on Titanium Implant Materials by Plasma Spraying, *J. Biomed. Mater. Res.*, 2000, **52**(2), p 333-337.
31. A. Meghwal, A. Anupam, B.S. Murty, C.C. Berndt, R.S. Kottada, and A.S.M. Ang, Thermal Spray High-Entropy Alloy Coatings: A Review, *J. Therm. Spray Technol.*, 2020, **29**(5), p 857-893.
32. P. Fauchais, M. Fukumoto, A. Vardelle, and M. Vardelle, Knowledge Concerning Splat Formation: An Invited Review, *J. Therm. Spray Technol.*, 2004, **13**(3), p 337-360.
33. K. Kim, S. Kuroda, and M. Watanabe, Microstructural Development and Deposition Behavior of Titanium Powder Particles in Warm Spraying Process: From Single Splat to Coating, *J. Therm. Spray Technol.*, 2010, **19**(6), p 1244-1254.
34. C.-J. Li and J.-L. Li, Evaporated-Gas-Induced Splashing Model for Splat Formation During Plasma Spraying, *Surf. Coat. Technol.*, 2004, **184**(1), p 13-23.
35. K. Kim, M. Watanabe, J. Kawakita, and S. Kuroda, Effects of Temperature of In-Flight Particles on Bonding and Microstructure in Warm-Sprayed Titanium Deposits, *J. Therm. Spray Technol.*, 2009, **18**(3), p 392-400.
36. K. Kim, M. Watanabe, K. Mitsuishi, K. Iakoubovskii, and S. Kuroda, Impact Bonding and Rebounding Between Kinetically Sprayed Titanium Particle and Steel Substrate Revealed by High-Resolution Electron Microscopy, *J. Phys. Appl. Phys.*, 2009, **42**(6), p 065304.
37. V. Pershin, M. Lufitha, S. Chandra, and J. Mostaghimi, Effect of Substrate Temperature on Adhesion Strength of Plasma-Sprayed Nickel Coatings, *J. Therm. Spray Technol.*, 2003, **12**(3), p 370-376.
38. J. Matejček, S. Sampath, and J. Dubsy, X-Ray Residual Stress Measurement in Metallic and Ceramic Plasma Sprayed Coatings, *J. Therm. Spray Technol.*, 1998, **7**(4), p 489-496.
39. H.R. Salimijazi, T.W. Coyle, J. Mostaghimi, and L. Leblanc, Microstructure and Failure Mechanism in As-Deposited, Vacuum Plasma-Sprayed Ti-6Al-4V Alloy, *J. Therm. Spray Technol.*, 2005, **14**(2), p 215-223.
40. H.R. Salimijazi, M. Raessi, J. Mostaghimi, and T.W. Coyle, Study of Solidification Behavior and Splat Morphology of Vacuum Plasma Sprayed Ti Alloy by Computational Modeling and Experimental Results, *Surf. Coat. Technol.*, 2007, **201**(18), p 7924-7931.

41. S. Sampath, X.Y. Jiang, J. Matejcek, A.C. Leger, and A. Vardelle, Substrate Temperature Effects on Splat Formation, Microstructure Development and Properties of Plasma Sprayed Coatings Part I: Case Study for Partially Stabilized Zirconia, *Mater. Sci. Eng. A*, 1999, **272**(1), p 181-188.
42. P.M. Bonutti, R. Pivec, K. Issa, B.H. Kapadia, S. Banerjee, M.A. Mont, and T.W. Bauer, Delamination of Tantalum Porous Coating From a TKA Due to Regional Dissemination of Debris, *Orthopedics*, 2013, **36**(8), p 600-604.
43. H. Zhou, Z. Liu, and L. Luo, Microstructural Characterization of Shrouded Plasma-Sprayed Titanium Coatings, *J. Manuf. Mater. Process.*, 2019, **3**(1), p 4.
44. M. Papakyriacou, Effects of Surface Treatments on High Cycle Corrosion Fatigue of Metallic Implant Materials, *Int. J. Fatigue*, 2000, **22**(10), p 873-886.

**Publisher's Note** Springer Nature remains neutral with regard to jurisdictional claims in published maps and institutional affiliations.